Inorganic Chemistry

Article

pubs.acs.org/IC

Links between the Crystal and Electronic Structure in the New Family of Unconventional Superconductors $A_2Cr_3As_3$ (A = K, Rb, Cs)

Pere Alemany*,† and Enric Canadell*,‡

†Departament de Química Física and Institut de Química Teórica i Computacional (IQTCUB), Universitat de Barcelona, Martí i Franquès 1, 08028 Barcelona, Spain

‡Institut de Ciència de Materials de Barcelona (CSIC), Campus de la UAB, 08193 Bellaterra, Spain

Supporting Information

ABSTRACT: The electronic structure of a new family of superconductors is examined through density functional theory calculations. In contrast with other quasi-1D superconductors, these phases exhibit a relatively complex electronic structure and the Fermi surface contains both 1D and 3D components. It is shown that cations have an almost nil influence on the electronic structure. The absence of a structural Peierls modulation is discussed, and the differences with the structurally related $M_2Mo_6Se_6$ (M = Tl, In, ...) superconductors are stressed. The large electron mass renormalization and the lack of clear correlation between $N(E_F)$ and T_c suggest the existence of strong electron correlations and an unconventional origin of the superconductivity.

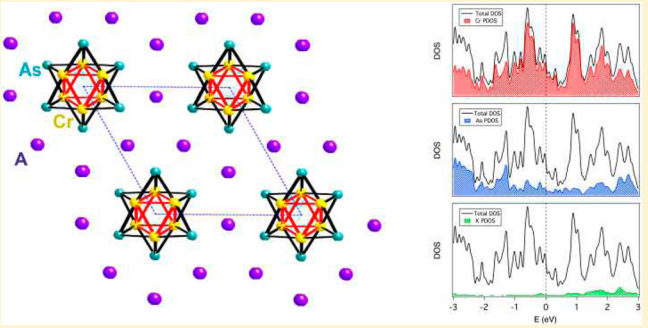

INTRODUCTION

Superconductivity remains one of the more fascinating yet elusive properties of solids. The lack of sound correlations between the structural and electronic features of different families of superconductors makes a rational approach to new materials with higher critical temperatures (T_c) extremely difficult. Low-dimensional superconductors rank among those having provided some of the more puzzling and exotic properties and in this respect, the question how low-dimensionality influences superconductivity has been and remains one of the central issues in modern condensed matter science. In particular, quasi-one-dimensional (quasi-1D) metals, with their strong tendency to undergo some kind of charge or spin density wave modulation as well as electronic localization, exhibit complex phase diagrams where superconductivity is in competition with several different ground states. The Bechgaard salts ($(TMTSF)_2X$; X = PF_6, ClO_4, ...),[1] the lithium purple bronze $Li_{0.9}Mo_6O_{17}$[2] and $Tl_2Mo_6Se_6$[3] are quasi-1D superconductors whose properties still challenge a full understanding.

Very recently, Cao and co-workers have reported[4] on a new family of structurally quasi-1D superconductors, $A_2Cr_3As_3$ with A = K, Rb, Cs. The main structural features of the $A_2Cr_3As_3$ crystals[4] (Figure 1a) are the $[Cr_6As_6]^{4-}$ chains (Figure 1b) running parallel to the crystal *c*-direction. In the crystal structure, each chain is surrounded by six equivalent neighbor chains leading to a hexagonal lattice. These $[Cr_6As_6]^{4-}$ chains are separated by cations that arrange in columns along the crystal *c*-direction. The critical temperature for bulk superconductivity varies from 6.1 K (A = K) to 4.8 K (A = Rb) and 2.2 K (A = Cs).[4] On the basis of different physical measurements,[5] like London penetration depth, magnetic susceptibility, NMR, and specific heat, unconventional superconductivity has been suggested for these phases.

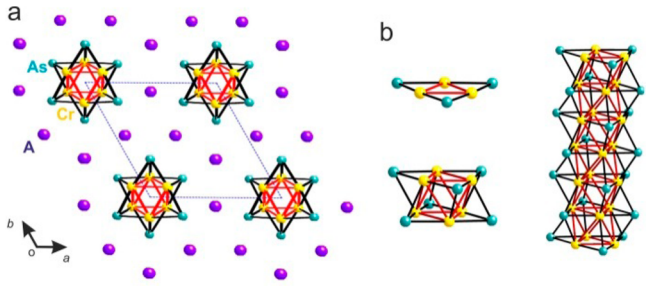

Figure 1. (a) Crystal structure of the $A_2Cr_3As_3$ superconductors along the *c*-direction. (b) Building up of the $[Cr_6As_6]^{4-}$ chains. Light blue, yellow, and purple spheres refer to As, Cr, and A atoms, respectively.

Many questions arise concerning the correlation between structural and electronic features of these systems. For instance, (i) Is there any relationship between T_c and the cation size? (ii) Why none of the usual electronic instabilities of quasi-1D systems, which often close the possibility to enter into the superconducting state, occur? (iii) What is the relationship with the structurally related family of quasi-1D metals $M_2Mo_6Se_6$ (M = Tl, In, Rb,..), two of which are superconductors (M = Tl, In) whereas others undergo metal to insulator transitions? Only two theoretical studies have been reported to date[6] for such phases,

Received: May 28, 2015
Published: July 31, 2015

DOI: 10.1021/acs.inorgchem.5b01207
Inorg. Chem. 2015, 54, 8029−8034

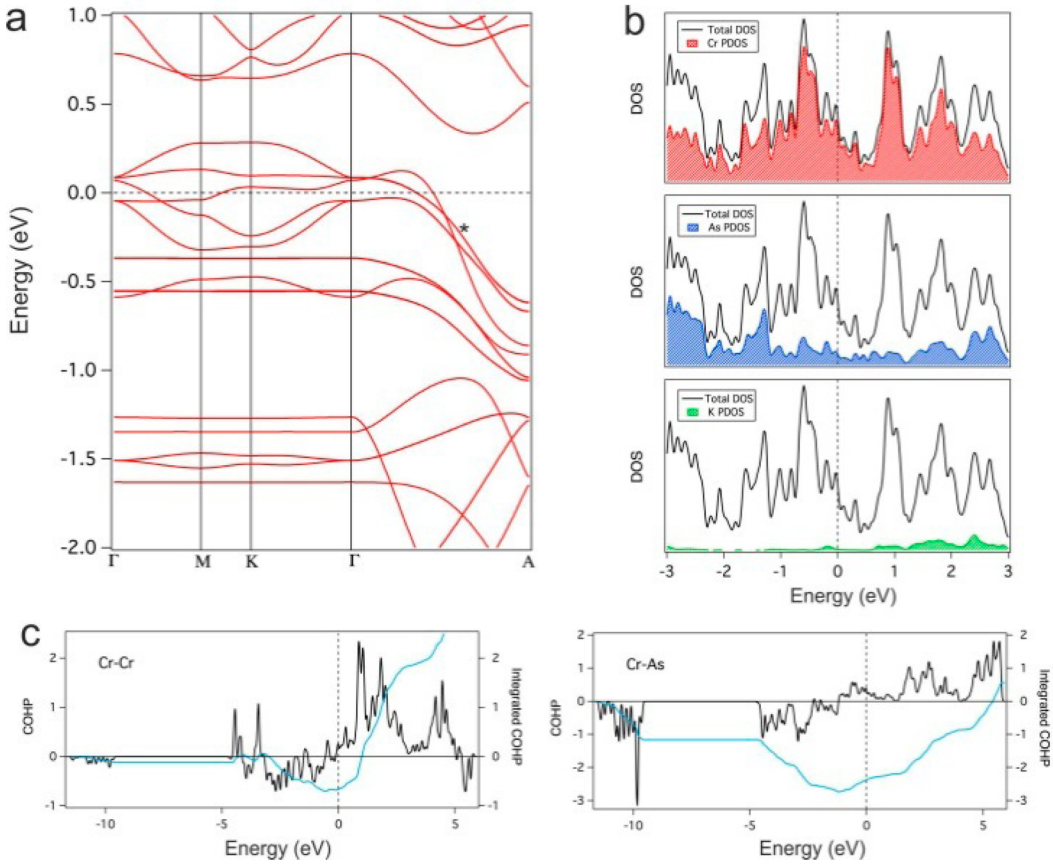

Figure 2. (a) Calculated band structure for $K_2Cr_3As_3$ where Γ = (0, 0, 0), M = (1/2, 0, 0), K = (1/3, 1/3, 0), A = (0, 0, 1/2), H = (1/3, 1/3, 1/2), and L = (1/2, 0, 1/2) in units of the reciprocal hexagonal lattice vectors. (b) Total and projected densities of states (Cr: red, As: blue and K: green) for $K_2Cr_3As_3$. (c) COHP (black) and integrated COHP (blue) curves for the Cr—Cr and Cr—As bonds. Negative/positive values indicate bonding/antibonding interactions.

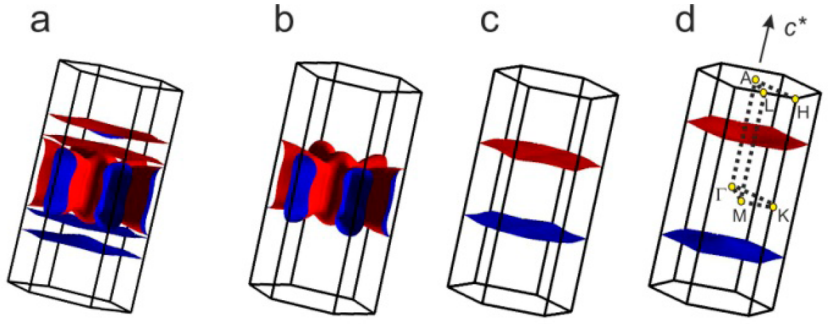

Figure 3. Calculated Fermi surface for $K_2Cr_3As_3$ (a) and its three separate components (b), (c), and (d).

but not much attention was paid to these questions. Yet these are important aspects to face in order to progress in our understanding of quasi-1D superconductors. Here we suggest some answers to these questions through a density functional theory (DFT) study of the three known members of this family as well as $Tl_2Mo_6Se_6$.

COMPUTATIONAL DETAILS

First-principles calculations were carried out using a numerical atomic orbitals DFT approach[7] developed for efficient calculations in large systems and implemented in the SIESTA code.[8−10] We have used the generalized gradient approximation (GGA) to DFT and, in particular, the functional of Perdew, Burke, and Ernzerhof.[11] Only the valence electrons are considered in the calculation, with the core being replaced by norm-conserving scalar relativistic pseudopotentials[12] factorized in the Kleinman−Bylander form.[13] We have used a split-valence double-ζ basis set including polarization orbitals as obtained with an energy shift of 10 meV for all atoms.[14] For Rb, Cs, and Tl, we have also included an additional semicore 4p (for Rb), 5p (for Cs), or 5d (for Tl) shell in the basis set. The energy cutoff of the real space integration mesh was 250 Ry, and the Brillouin zone was sampled using grids[15] of (10 × 10 × 10) *k*-points for the calculation of the density matrix, (10 × 10 × 100) *k*-points for the calculation of the densities of states at the Fermi level and (20 × 20 × 20) *k*-points for the calculation of the Fermi surface. All calculations presented were performed using the experimental crystal structures.[3b,4]

RESULTS AND DISCUSSION

The basic building block of the $[Cr_6As_6]^{4-}$ chains is a Cr_3As_3 triangular cluster (Figure 1b) which repeats along the chain with

DOI: 10.1021/acs.inorgchem.5b01207
Inorg. Chem. 2015, 54, 8029−8034

alternating directions. The two consecutive triangles are not fully equivalent and have slightly different Cr—Cr and Cr—As distances so that the repeat unit of the chain is a Cr_6As_6 unit composed by two alternated triangles (Figure 1b and the Supporting Information, SI, for additional structural discussion). The calculated band structure for $K_2Cr_3As_3$ is shown in Figure 2a. The band marked with an asterisk along Γ−A is doubly degenerate. There are three bands crossing the Fermi level along this line, i.e., along the chain direction. In addition, one band also cuts the Fermi level in the Γ−M−K plane (note that the crossing just below the Fermi level along the Γ−M line is not allowed for most points of the Brillouin zone so that we must consider that only three bands cross the Fermi level). Consequently, the Fermi surface should contain two 1D components and one 3D component. The calculated Fermi surface (FS) is shown in Figure 3. Two of the components (Figure 3c and d) are indeed 1D although, as better seen in Figure 3a, one of them has a non-negligible warping around the central part. As a matter of fact, the 3D FS of Figure 3b is reminiscent of a pair of warped planes perpendicular to *c* somewhat distorted to connect the two sections, clearly pointing out the quasi-1D nature of the structure. The calculated density of states (DOS) as well as the projected DOS (PDOS) associated with Cr, As, and K are reported in Figure 2b. The DOS around the Fermi level is heavily concentrated in the Cr atoms with a relatively small contribution of the As atoms and an almost negligible participation of the K atoms. This suggests a weak influence of the cation on the electronic structure.

Looking for the nature of the states around the Fermi level we have calculated the crystal orbital Hamilton population (COHP)[16] curves for the Cr—Cr and Cr—As bonds. From these curves (Figure 2c) it can be deduced that the bands in the region from −1 to 0 eV are mainly Cr—Cr bonding bands, while those above the Fermi level have soon a strong Cr—Cr antibonding character. Further analysis shows that at the Fermi level the Cr—Cr interactions within each triangle are bonding whereas those between triangles are antibonding. This is understandable because the Fermi level hits the top of bands dispersive along the chain direction and these levels must consequently be antibonding between the triangular units. However, the bands are globally Cr—Cr bonding because of the larger bonding character within the triangles. The COHP curve for the Cr—As bonds shows that in the region around the Fermi level, we have basically nonbonding interactions with a small positive (antibonding) character. Note that the metal−metal bonding is practically optimized for the electron count in these phases. To gain a better insight we carried out a fatband analysis of the band structure (SI Figure S5). The three partially filled bands in Figure 2a are mainly built from a complex mixing of the d_{z2}, d_{x2-y2}, and d_{xy} orbitals of Cr. However, with this sole information it is not clear why the bands near the Fermi level exhibit the shape shown in Figure 2a. Because of the extensive metal−metal and metal−arsenic bonding, we must look deeper into the wave functions for selected *k*-points. The five bands around the Fermi level can be separated along the Γ−A line as two pairs of doubly degenerate bands and one nondegenerate band. The two pairs of degenerate bands mostly originate from the pair of degenerate orbitals of the triangular cluster shown in **1**[17] (only the metal contribution is shown for simplicity). The nondegenerate orbital originates from the orbital shown in **2**. Since there are two triangular units per unit cell, in-phase and out-of-phase combinations of these orbitals can be built. Because of the hexagonal symmetry some of the bands can cross along the symmetry lines shown in Figure 2a but inside the Brillouin zone they all undergo a strong mixing which essentially describes the metal−metal and metal−arsenic interactions between triangular units. The out-of-phase combination of **2**, strongly hybridized with a combination of d_{x2-y2} orbitals of the same symmetry, stays at lower energies, whereas the four combinations of orbitals **1** and the second combination based on **2** lead to the set of five bands around the Fermi level. The three partially filled bands are built from the in-phase combination of the orbitals in **1** and **2** (with a smaller yet significant participation of As). Note however that in a significant part of the Brillouin zone the bands based on **1** also mix in a non-negligible way with the levels shown in **3**. Thus, the three partially filled bands acquire d_{z2} character, and this is why all bands exhibit a very substantial dispersion along the chain direction. At the same time, the four bands originating from orbitals **1**, with strong in-plane character, can exhibit some dispersion in the interchain directions mostly through the As contribution.

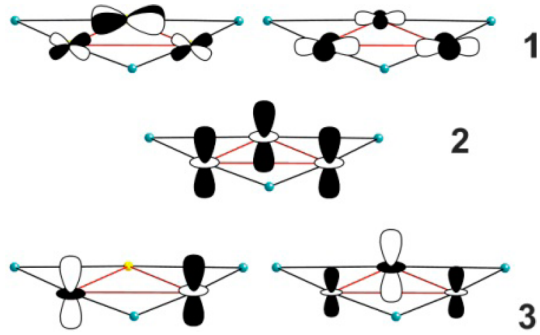

At this point, it is interesting to compare these results with those for the structurally related quasi-1D superconductor $Tl_2Mo_6Se_6$. The main structural difference with the $A_2Cr_3As_3$ phases is that the two triangular building blocks of the $[Mo_6Se_6]^{2-}$ chains are equivalent and the packing of the chains is slightly different because of the different number of cations in-between (see SI). The calculated band structure is shown in Figure 4a. Substitution of Se for As leads to an increase of six electrons per M_6X_6 unit in the Mo_6Se_6 chains, although the different cation content leads to only four additional electrons per M_6X_6 unit in $Tl_2Mo_6Se_6$. As a consequence, the Fermi level is now in a completely different region. Another important difference is the considerably large increase in the metal−metal interactions from Cr to Mo. This feature strongly increases the

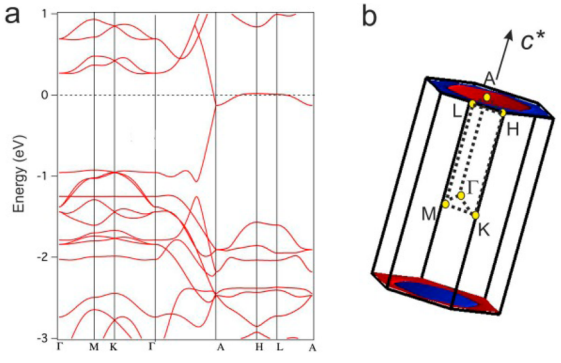

Figure 4. (a) Calculated band structure for $Tl_2Mo_6Se_6$, where Γ = (0, 0, 0), M = (1/2, 0, 0), K = (1/3, 1/3, 0), A = (0, 0, 1/2), H = (1/3, 1/3, 1/2), and L = (1/2, 0, 1/2) in units of the reciprocal hexagonal lattice vectors. (b) Fermi surface calculated for $Tl_2Mo_6Se_6$.

DOI: 10.1021/acs.inorgchem.5b01207
Inorg. Chem. 2015, 54, 8029−8034

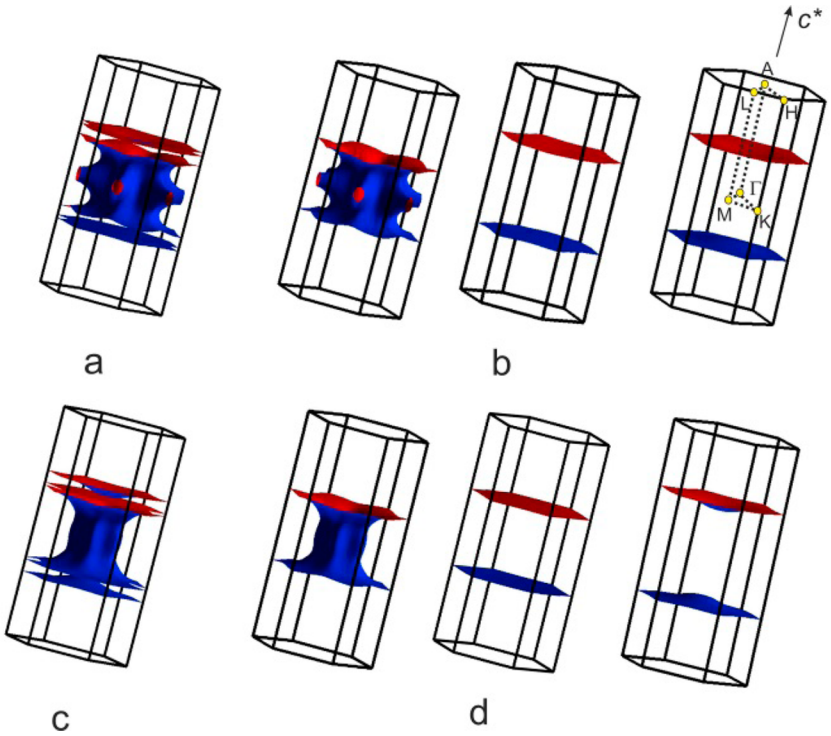

Figure 5. Calculated Fermi surface for $Rb_2Cr_3As_3$ (a) and $Cs_2Cr_3As_3$ (c). The three separate components of the Fermi surface for $Rb_2Cr_3As_3$ (b) and $Cs_2Cr_3As_3$ (d).

interactions along the chain and more especially the width of bands based on the d_{xz} and d_{yz} orbitals. This is the case of the highly dispersive and partially filled bands around the Fermi level in Figure 4a, the lower of which undergoes an avoided crossing around −1 eV. With four electrons more per repeat unit, the partially filled bands in $A_2Cr_3As_3$ are now completely full and two electrons remain to fill the next band. Because of the stronger Mo−Mo interactions, the highest occupied band in $Tl_2Mo_6Se_6$ is strongly lowered. This could have resulted with a band gap at the Fermi level and thus, with a semiconducting behavior if the chains were identical to those of $A_2Cr_3As_3$. However, the two triangles of the unit cell are fully equivalent in $Tl_2Mo_6Se_6$. This leads to a screw rotational symmetry along *c* and to the degeneracy of the two highly dispersive $d_{xz/yz}$ based bands at A, so that the system is metallic. The weak but non-negligible dispersion of this pair of bands along directions perpendicular to the chain due to the interaction with the Tl atoms leads to the flat still slightly warped Fermi surface of Figure 4b. All these results are in excellent agreement with recent first-principles calculations for this system.[3a] It is worth pointing out that the bands composed by orbitals **1** (the four dispersive bands in the Γ−M−K plane between −1.0 and −1.5 eV) have a similar dispersion in the Γ−M−K plane as in the $A_2Cr_3As_3$ compounds, although in this case this is not a relevant issue since they are completely filled. In short, the first vs second row nature of the metals, the different electron counting and a subtle structural detail, all conspire in making two structurally similar families of compounds completely different from the electronic viewpoint.

We have also carried out similar calculations for $Rb_2Cr_3As_3$ and $Cs_2Cr_3As_3$, and the results are quite similar to those obtained for $K_2Cr_3As_3$. There is however a difference. In both compounds the nondegenerate band along Γ-A is slightly lowered in energy and does not cut the Fermi level along this direction (Figure S4). As a result, the 3D component of the Fermi surface is empty in a very large region around the *c** axis (see Figure 5). The shape of this 3D component of the FS is thus, according to our calculations, different in the three compounds. Magnetoresistance studies should be helpful in exploring such differences. That such changes are responsible or not for differences in the physical properties of these phases is something that remains to be scrutinized. Note however that the difference between the K and the Rb/Cs phases results from the fact that the dispersion along the *c*-direction decreases a bit in the latter and thus it is an intrachain effect. This means that the difference between the K and the Rb/Cs phases is maybe related to the different degree of dimerization of the chain, i.e., the difference between two successive Cr_3As_3 triangular units of the $[Cr_6As_6]^{4-}$ chains. This would be an interesting aspect to take into account if the magnetoresistance studies confirm the noted subtle differences. It is clear however that the actual shape of the 3D FS of these systems critically depends of many factors. An interesting question is that of the role of the interchain interactions, because the DOS plot in Figure 2b seems to indicate that cations have a very low participation in the region around the Fermi level, and the interchain As—As distances are long (the shortest As—As distances between neighboring chains are 5.009/5.080 Å, 4.954/5.291 Å, and 5.368/5.511 Å for $K_2Cr_3As_3$, $Rb_2Cr_3As_3$, and $Cs_2Cr_3As_3$, respectively) which seem to rule out strong direct through-space interactions. To shed some light into this question, we have performed calculations in which the cations have been replaced by a positive background of uniformly distributed positive charge (SI Figure S6). Although the overall dispersion in the Γ−M−K plane of the group of bands in the region from −0.2 to +0.2 eV around the Fermi level is reduced when the K atoms are removed from the calculation, they do not become completely dispersionless. This only happens when the chains are further separated. Thus, we conclude that interactions through the cations and residual direct interactions, probably due

DOI: 10.1021/acs.inorgchem.5b01207
Inorg. Chem. 2015, 54, 8029−8034

to the quite diffuse character of the As orbitals, are at work. Thus, we conclude that the dispersion perpendicular to the chain direction, which is weak though significant because the Fermi level hits one of the three bands in the Γ−M−K plane, results from the addition from several very small contributions, and consequently it will be difficult to control, for instance with pressure. Although the existence of two 1D components of the FS seems to be a robust feature, it is clear that the shape of the 3D component results from a delicate combination of weak contributions. Under such circumstances, it is clear that physical and chemical pressures may have very different consequences for the electronic structure and physical behavior of the phases. Kong et al.[5b] have reached a similar conclusion concerning the effect on the superconductivity.

The calculated densities of states at the Fermi level, $N(E_F)$, for $K_2Cr_3As_3$, $Rb_2Cr_3As_3$, and $Cs_2Cr_3As_3$ are 6.27, 5.56, and 5.52 electrons per eV per formula unit, respectively. Let us note that special care is needed in order to have well converged values for $N(E_F)$. From these numbers, we can conclude that there is apparently no relationship between $N(E_F)$ and the cation size. The evolution of $N(E_F)$ is consistent with the fact that the non degenerate band along Γ−A does not cut the Fermi level along this direction in $Rb_2Cr_3As_3$ and $Cs_2Cr_3As_3$, in contrast with the case of $K_2Cr_3As_3$. Taking the theoretical and experimental values for $K_2Cr_3As_3$, a large electron mass renormalization of ∼4.5 is found. The decrease of $N(E_F)$ from $K_2Cr_3As_3$ to $Rb_2Cr_3As_3$ is consistent with the decrease in T_c. However, whereas T_c is reduced by 42% from $Rb_2Cr_3As_3$ to $Cs_2Cr_3As_3$, the $N(E_F)$ is kept practically constant. Both the large electron mass renormalization and the lack of clear correlation between the $N(E_F)$ and T_c values point toward the existence of strong correlations and an unconventional origin of the superconductivity.

Since two open 1D FS occur for the three systems of this family, we should now consider why they do not undergo the usual charge or spin density wave modulations of quasi-1D systems. Jiang et al.[6a] have found that the imaginary part of the susceptibility exhibits strong peaks at Γ, which suggests ferromagnetic fluctuations. This makes unlikely the possibility of a spin density wave. What remains to be understood is why the system avoids a structural modulation of the charge density wave type. Here we must note that even in the $M_2Mo_6Se_6$ quasi-1D systems, which provides a considerably simpler and more likely case, such modulation does not seem to be very favorable since it does not occur in $Tl_2Mo_6Se_6$, for instance. The metallic chains are probably quite stiff because of the extensive metal−metal and metal ligand bonding within and between triangular units. In the present case, the FS has three components. Only the two flat 1D components can have a large contribution to the susceptibility. We remind that one of them is quite warped around the c^* axis. Consequently, an interband nesting mechanism such as that occurring in the blue bronzes which would simultaneously destroy the two 1D components[19] is not likely. Thus, only an intraband nesting mechanism destroying the very flat 1D component seems to be reasonable in this case but this would leave a large part of the FS unaltered and should not provide a strong driving force for the modulation. In addition, there are also chemical reasons against such modulation. As our analysis of the bonding in $K_2Cr_3As_3$ suggests, around the Fermi level there is a strong hybridization between the d_{z2} orbitals pointing along the chain and implicated in the Cr—Cr intertriangles interactions, and the d_{x2-y2}/d_{xy} orbitals strongly implicated in the Cr—Cr intratriangle bonding. Opening a gap in the c^* direction would only slightly stabilize the intertriangle Cr—Cr bonds because the gap would open not far from the top of the band where antibonding interactions dominate. Because of the strong hybridization above-mentioned, such weak stabilization of the intertriangle bonding would be accompanied by a destabilization of the intratriangle Cr—Cr bonding making the driving force for the modulation extremely small or nonexistent.

CONCLUSIONS

We thus conclude that, in contrast with usual quasi-1D superconductors, the $A_2Cr_3As_3$ (A = K, Rb, Cs) phases exhibit a relatively complex electronic structure around the Fermi level. The Fermi surface contains two 1D and one 3D components. The present study suggests that cations and the separation between the $[Cr_6As_6]^{4-}$ chains have an almost nil influence on the electronic structure. The differences between the three members of the family must arise because of intrachain changes. The large electron mass renormalization and the lack of a clear correlation between the $N(E_F)$ and T_c values suggest the existence of strong electron correlations and an unconventional origin of the superconductivity. The absence of a Peierls-type modulation seems to originate from the fact that the possible intraband nesting mechanism would leave a large portion of the Fermi surface unaltered, and because of the strong hybridization between Cr d orbitals around the Fermi level, it would be associated with a weak stabilization of bonding along the chain direction and a larger destabilization of bonding within the triangular units. A comparison with the structurally related quasi-1D superconductor $Tl_2Mo_6Se_6$ shows that the first vs second row nature of the metals, the different electron counting and a subtle structural detail, the presence of two equivalent or different M_3X_3 triangular units, work together in making two structurally similar families of compounds very different from the electronic viewpoint.

ASSOCIATED CONTENT

Supporting Information

(1) Additional structural discussion and (2) band structures and fatband analysis for the $A_2Cr_3As_3$ compounds; and additional tables or figures. The Supporting Information is available free of charge on the ACS Publications website at DOI: 10.1021/acs.inorgchem.5b01207.

AUTHOR INFORMATION

Corresponding Authors

*E-mail: p.alemany@ub.edu (P.A.).
*E-mail: canadell@icmab.es (E.C.).

Notes

The authors declare no competing financial interest.

ACKNOWLEDGMENTS

This work was supported by MINECO (Spain) through Grant FIS2012-37549-C05-05 and Generalitat de Catalunya (2014 SGR301 and XRQTC).

REFERENCES

(1) (a) Jérome, D. *Science* **1991**, *252*, 1509. (b) Bechgaard, K.; Jacobsen, C. S.; Mortensen, K.; Pederson, J. H.; Thorup, N. *Solid State Commun.* **1980**, *33*, 1119−1125.

(2) (a) Chudzinski, P.; Jarlborg, T.; Giamarchi, T. *Phys. Rev. B: Condens. Matter Mater. Phys.* **2012**, *86*, 075147. and references therein. (b) Greenblatt, M.; McCarroll, W. H.; Neifeld, R.; Croft, M.; Waszczak. *Solid State Commun.* **1984**, *51*, 671−674.

DOI: 10.1021/acs.inorgchem.5b01207
Inorg. Chem. 2015, 54, 8029−8034

(3) (a) Petrovic, A. P.; Lortz, R.; Santi, G.; Decroux, M.; Monnard, H.; Fischer, Ø.; Boeri, L.; Andersen, O. K.; Kortus, J.; Salloum, D.; Gougeon, P.; Potel, M. *Phys. Rev. B: Condens. Matter Mater. Phys.* **2010**, *182*, 235128. and references therein. (b) Potel, M.; Chevrel, R.; Sergent, M.; Armici, J. C.; Decroux, M.; Fischer, Ø. *Acta Crystallogr., Sect. B: Struct. Crystallogr. Cryst. Chem.* **1980**, *B36*, 1545−1548.
(4) (a) Bao, J.-K.; Liu, J.-Y.; Ma, C.-W.; Meng, Z.-H.; Tang, Z.-T.; Sun, Y.-L.; Zhai, H.-F.; Jiang, H.; Bai, H.; Feng, C.-M.; Xu, Z.-A.; Cao, G.-H. *Phys. Rev. X* **2015**, *5*, 011013. (b) Tang, Z.-T; Bao, J.-K.; Liu, Y.; Sun, Y.-L.; Ablimit, A.; Zhai, H.-F.; Jiang, H.; Feng, C.-M.; Xu, Z.-A.; Cao, G.-H. *Phys. Rev. B: Condens. Matter Mater. Phys.* **2015**, *91*, 020506(R). (c) Tang, Z.-T; Bao, J.-K.; Wang, Z.; Bai, H.; Jiang, H.; Liu, Y.; Zhai, H.-F.; Meng, C.-M.; Xu, Z.-A.; Cao, G.-H. *Sci. China Mater.* **2015**, *58*, 16−20.
(5) (a) Pang, G. M.; Smidman, M.; Jiang, W. B.; Bao, J. K.; Weng, Z. F.; Wang, Y. F.; Jiao, L.; Zhang, J. L.; Cao, G. H.; Yuan, H. Q. *Phys. Rev. B: Condens. Matter Mater. Phys.* **2015**, *91*, 220502(R). (b) Kong, T.; Bud'ko, S. L.; Canfield, P. *Phys. Rev. B: Condens. Matter Mater. Phys.* **2015**, *91*, 020507(R). (c) Zhi, H. Z.; Imai, T.; Ning, F. L.; Bao, J. K.; Cao, G.-H. *Phys. Rev. Lett.* **2015**, *114*, 147004. (d) Adroja, D. T.; Bhattacharyya, A.; Telling, M.; Feng, Y.; Smidman, M.; Pan, B.; Zhao, J.; Hillier, A. D.; Pratt, F. L.; Strydom, A. M. Searching for triplet superconductivity in the Quasi-One-Dimensional $K_2Cr_3As_3$ **2015**, arXiv:1505.05743v1. arXiv.org e-Print archive://arxiv.org/abs/1505.05743 (accessed July 23, 2015).
(6) (a) Jiang, H.; Cao, G.; Cao, C. Electronic structure of quasi-one-dimensional superconductor $K_2Cr_3As_3$ from first-principles calculations. **2014**, arXiv:1412.1309v1. arXiv.org e-Print archive://arxiv.org/abs/1412.1309 (accessed July 23, 2015). (b) Wu, X.; Le, C.; Yuan, J.; Fan, H.; Hu, J. *Chin. Phys. Lett.* **2015**, *32*, 057401.
(7) Hohenberg, P.; Kohn, W. *Phys. Rev.* **1964**, *136*, B864−B871. Kohn, W.; Sham, L. J. *Phys. Rev.* **1965**, *140*, A1133−A1138.
(8) Soler, J. M.; Artacho, E.; Gale, J. D.; García, A.; Junquera, J.; Ordejón, P.; Sánchez-Portal, D. *J. Phys.: Condens. Matter* **2002**, *14*, 2745−2779.
(9) For more information on the SIESTA code visit: http://departments.icmab.es/leem/siesta/.
(10) For a review on applications of the SIESTA approach in materials science, see: Sánchez-Portal, D.; Ordejón, P.; Canadell, E. *Structrure and Bonding (Berlin)* **2004**, *113*, 103−170.
(11) Perdew, J. P.; Burke, K.; Ernzerhof, M. *Phys. Rev. Lett.* **1996**, *77*, 3865−3868.
(12) Troullier, N.; Martins, J. L. *Phys. Rev. B: Condens. Matter Mater. Phys.* **1991**, *43*, 1993−2006.
(13) Kleinman, L.; Bylander, D. M. *Phys. Rev. Lett.* **1982**, *48*, 1425−1428.
(14) Artacho, E.; Sánchez-Portal, D.; Ordejón, P.; García, A.; Soler, J. M. *Phys. Status Solidi B* **1999**, *215*, 809−817.
(15) Monkhorst, H. J.; Pack, J. D. *Phys. Rev. B* **1976**, *13*, 5188−5192.
(16) Dronskowski, R. *Computational Chemistry of Solid State Materials*; Wiley-VCH: Weinheim, 2005.
(17) For a discussion of the orbitals of the triangular cluster, see: (a) Hughbanks, T. R.; Hoffmann, R. *J. Am. Chem. Soc.* **1983**, *105*, 1150−1162. (b) Hughbanks, T. R.; Hoffmann, R. *Inorg. Chem.* **1982**, *21*, 3578−3580.
(18) Grüner, G. *Density Waves in Solids*; Addison-Wesley: Reading, MA, 1994.
(19) Canadell, E.; Whangbo, M.-H. *Chem. Rev.* **1991**, *91*, 965−10.

DOI: 10.1021/acs.inorgchem.5b01207
Inorg. Chem. 2015, 54, 8029−8034